

# Synergistic dual catalytic system and kinetics for the alcoholysis of poly(lactic acid)

Lamberti, Fabio; Ingram, Andy; Wood, Joe

DOI:

[10.3390/pr9060921](https://doi.org/10.3390/pr9060921)

License:

Creative Commons: Attribution (CC BY)

*Document Version*

Publisher's PDF, also known as Version of record

*Citation for published version (Harvard):*

Lamberti, F, Ingram, A & Wood, J 2021, 'Synergistic dual catalytic system and kinetics for the alcoholysis of poly(lactic acid)', *Processes*, vol. 9, no. 6, 921. <https://doi.org/10.3390/pr9060921>

[Link to publication on Research at Birmingham portal](#)

## General rights

Unless a licence is specified above, all rights (including copyright and moral rights) in this document are retained by the authors and/or the copyright holders. The express permission of the copyright holder must be obtained for any use of this material other than for purposes permitted by law.

- Users may freely distribute the URL that is used to identify this publication.
- Users may download and/or print one copy of the publication from the University of Birmingham research portal for the purpose of private study or non-commercial research.
- User may use extracts from the document in line with the concept of 'fair dealing' under the Copyright, Designs and Patents Act 1988 (?)
- Users may not further distribute the material nor use it for the purposes of commercial gain.

Where a licence is displayed above, please note the terms and conditions of the licence govern your use of this document.

When citing, please reference the published version.


## Take down policy

While the University of Birmingham exercises care and attention in making items available there are rare occasions when an item has been uploaded in error or has been deemed to be commercially or otherwise sensitive.

If you believe that this is the case for this document, please contact [UBIRA@lists.bham.ac.uk](mailto:UBIRA@lists.bham.ac.uk) providing details and we will remove access to the work immediately and investigate.

## Article

# Synergistic Dual Catalytic System and Kinetics for the Alcoholysis of Poly(Lactic Acid)

Fabio M. Lamberti, Andy Ingram and Joseph Wood \* 

School of Chemical Engineering, University of Birmingham, Edgbaston, Birmingham B15 2TT, UK; fxl876@student.bham.ac.uk (F.M.L.); A.Ingram@bham.ac.uk (A.I.)

\* Correspondence: J.Wood@bham.ac.uk

**Abstract:** Plastic pollution is a global issue that is approaching crisis levels as plastic production is projected to reach 1.1 GT annually by 2050. The bioplastic industry along with a circular production economy are solutions to this problem. One promising bioplastic polylactic acid (PLA) has mechanical properties comparable to polystyrene (PS), so it could replace PS in its applications as a more environmentally sustainable material. However, since the bioplastic PLA also suffers from long biodegradation times in the environment, to ensure that it does not add to the current pollution problem, it should instead be chemically recycled. In this work, PLA was chemically recycled via alcoholysis, using either methanol or ethanol to generate the value-added products methyl lactate and ethyl lactate respectively. Two catalysts, zinc acetate dihydrate (ZnAc) and 4-(dimethylamino)pyridine (DMAP), were tested both individually and in mixtures. A synergistic effect was exhibited on the reaction rate when both catalysts were used in an equal ratio. The methanolysis reaction was determined to be two-step, with the activation energy estimated to be 73 kJ mol<sup>-1</sup> for the first step and 40.16 kJ mol<sup>-1</sup> for the second step. Both catalysts are cheap and commercially available, their synergistic effect could be exploited for large-scale PLA recycling.

**Keywords:** poly(lactic acid); chemical recycling; alcoholysis; zinc acetate dihydrate; 4-(dimethylamino)pyridine; synergistic catalytic system



**Citation:** Lamberti, F.M.; Ingram, A.; Wood, J. Synergistic Dual Catalytic System and Kinetics for the Alcoholysis of Poly(Lactic Acid). *Processes* **2021**, *9*, 921. <https://doi.org/10.3390/pr9060921>

Academic Editors: Alazne Gutiérrez and Roberto Palos

Received: 29 April 2021

Accepted: 21 May 2021

Published: 24 May 2021

**Publisher's Note:** MDPI stays neutral with regard to jurisdictional claims in published maps and institutional affiliations.



**Copyright:** © 2021 by the authors. Licensee MDPI, Basel, Switzerland. This article is an open access article distributed under the terms and conditions of the Creative Commons Attribution (CC BY) license (<https://creativecommons.org/licenses/by/4.0/>).

## 1. Introduction

Petroleum-derived thermoplastics have become indispensable tools in our everyday lives. Their total production had been projected to reach 1.1 GT annually by 2050, while the total cumulative weight of plastic production since 1950 is projected to reach 34 GT [1–3]. Their characteristically high mechanical and barrier properties combined with a low bulk density and inertness make them superior materials for a wide variety of applications. A downside to petroleum thermoplastics is their extremely long biodegradation time, which causes unrestricted environmental damage when disposed of incorrectly [3,4]. By implementing a circular economy the long biodegradation times of petroleum plastics becomes irrelevant. In theory, postconsumer plastics could all be collected and recycled to products of equivalent functionality; if done correctly, a circular approach would have an immense economic and environmental advantage [1,5,6]. A circular approach would typically involve the less energy-intensive reuse and mechanical recycling stages first; this could be repeated until the quality of the recycled plastic has diminished to the point that it can no longer meet the requirements of its application [4,7]. From here, low-grade plastic should be recycled by a chemical method of the lowest activation energy. Chemical recycling can be used to generate value-added products or virgin grade monomers. Then, the pure monomers could be used for repolymerisation, which lowers the requirement of petroleum for virgin grade polymer synthesis [8].

Unfortunately, a circular economy is still not implemented for the majority of plastics; by 2025, an estimated 100 MT of plastic will have entered the oceans [6]. In the marine

environment, non-biodegradable plastics such as high-density polyethylene (HDPE) and polypropylene (PP) have a maximum weight loss of 0.8% and 0.6% respectively in six months [9]. Oceanic plastic debris slowly biodegrade and generate microplastics; both plastics and microplastics cause widespread contamination of marine ecosystems negatively impacting the health of its organisms. Alarmingly, microplastics have been shown to inhibit the growth of phytoplankton and marine plants, which account for over half of the atmospheric stock of oxygen. Therefore, oceanic plastic pollution could have a dire consequences for global warming and climate change [10,11].

The emerging bioplastic industry could act as a possible solution to these problems [12,13]. Second-generation bioplastics have a smaller carbon footprint than petroleum plastics; additionally, some bioplastics possess very high biodegradability, making them a more environmentally sustainable material [14]. One of the most important bioplastics, PLA, makes up a growing 10% of the bioplastic market; it has mechanical properties similar to PS and could replace it in many applications [14,15]. Although PLA is marketed as a bioplastic, its rate of biodegradation is relatively slow; after one year in the marine environment, PLA only degrades by approximately 8% [13,16]. In soil, the rate of weight loss of pure PLA is  $\approx 0\%$  per year, which is partly due to the fact that only  $\approx 0.04\%$  of microorganism colonies in soil are capable of degrading PLA [17,18]. However, in a controlled composting environment with high temperature and humidity, PLA will fully degrade in less than 90 days [19].

The chemical recycling of PLA is a promising alternative to limited mechanical recycling and biodegradation [20]. One of the most promising chemical recycling methods for depolymerising PLA is via alcoholysis; this route can be carried out at milder operating conditions than other chemical methods and has the additional benefit of generating a value-added product alkyl lactate (AL) [21–24]. ALs are employed in several industries and are considered green solvents due to their biodegradability and low toxicity [25]. ALs have an estimated market value of £12 billion, and their use is expected to increase in the future [23,26]. Notably, a circular economy approach is possible, since recovered AL from postconsumer PLA can be converted to lactide, as shown below in Figure 1 [27,28]. Lactide is the precursor for ring opening polymerisation, which generates virgin grade PLA. Zn(II) complexes have previously been shown to be highly active for both the polymerisation and depolymerisation of PLA [22,29]. It is worth noting that it is possible to chemically recycle PLA directly to lactide; this is a more useful route if the regeneration of virgin PLA is desired over obtaining the value-added ALs [30]. In this work, methyl lactate (MeLa) and ethyl lactate (EtLa) were produced from the catalysed alcoholysis of PLA with the corresponding alcohol. The aim of this work is to make PLA alcoholysis more applicable to an industrial setting; to this end, cheap commercially available catalysts were employed.

Zinc acetate dihydrate (ZnAc) has been widely reported for the transesterification of polyesters, and it has been shown to be effective as a catalyst in both the glycolysis and methanolysis of polyethylene terephthalate (PET) [21,31–33]. Additionally, ZnAc has been shown to be highly active for the alcoholysis of PLA, and it can even be used as a pretreatment to depolymerise unwanted PLA in a PET recycling stream [30,34]. Likewise, 4-(dimethylamino)pyridine (DMAP) has been shown to be an effective transesterification catalyst and has been employed in PLA alcoholysis [35–37]. As both ZnAc and DMAP are commercially available, they can be bought instead of synthesised, which is an advantage over the Zn(II) catalysts used in our previous paper [22]. Both catalysts were tested individually and in different mixtures at the same total weight percentage relative to PLA weight. The mixture of catalysts produced the best results, generating a final conversion of MeLa in the quickest times; the highest initial reaction rate was achieved using an equal ratio of both catalysts. Since reactions proceeded faster and with higher selectivity for the product when both catalysts were employed together instead of either alone, it suggests that there is a synergistic effect between the two catalysts for PLA alcoholysis.

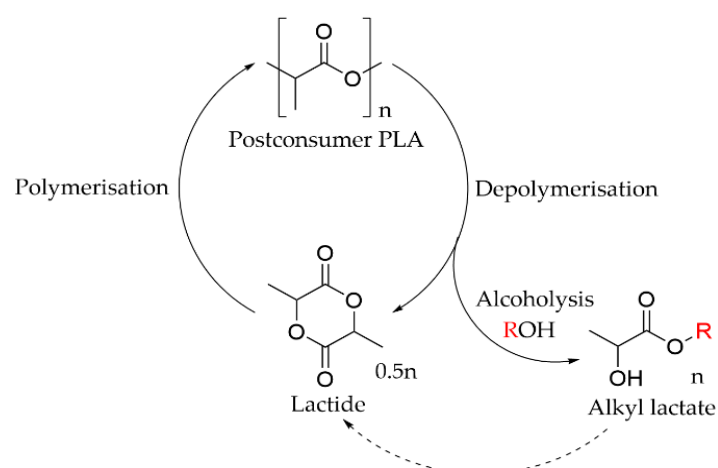


**Figure 1.** General scheme for the circular economy of PLA via chemical recycling. Alcoholysis allows for the generation of the value-added product AL.

Over the past two decades, the use of dual catalyst systems consisting of transition metal complexes alongside an organocatalyst has received increasing attention [38–40]. Careful selection of synergistic catalysts can cause unprecedented reactivities, which would not be accessible using either catalyst alone. Romiti et al. discussed that there are four types of dual-catalytic reactions: Type I is for fully cooperative catalysts, where each catalyst reacts exclusively with only one substrate; Type II is for partially cooperative catalysts, where using either of the catalysts alone would result in the formation of the desired product, but at a significantly slower rate and/or with lower stereoselectivity compared to using both catalysts; Type III is for partially cooperative catalysts, but in this case, one of the catalysts used alone would result in slow and/or minimally enantioselective reaction, while the other catalyst alone would cause substrate decomposition and the formation of undesirable side products; Type IV is for non-cooperative catalysts that require correct synchronisation in order to be useful [40].

In this work, we present the synergistic effect of ZnAc and DMAP. Specifically, we found that the highest initial reaction rate is achieved when the two catalysts are used in an equal ratio; at the same temperature, the methanolysis of PLA achieves a final yield of AL > 97% in a shorter time in comparison with ethanolysis of PLA; a higher temperature improves both the selectivity and yield of AL; the activation energy for step 1 and 2 of PLA methanolysis was estimated at  $73 \text{ kJ mol}^{-1}$  and  $40.16 \text{ kJ mol}^{-1}$ , respectively.

## 2. Materials and Methods

### 2.1. Materials

PLA pellets, supplied by NatureWorks (Ingeo™ 6202D, average molecular weight number 44,350 ( $\text{g mol}^{-1}$ )) were used without pretreatment. All reactants were HPLC grade: Methanol (MeOH)  $\geq 99.8\%$ , ethanol (EtOH)  $\geq 99.8\%$ , tetrahydrofuran (THF, HPLC grade,  $\geq 99.9\%$  without inhibitor) were purchased from Fisher scientific. ZnAc and DMAP were purchased from Sigma-Aldrich (St. Louis, MO, USA). All chemicals were used as received. Helium CP grade ( $\geq 99.999\%$  purity), nitrogen (oxygen-free,  $\geq 99.998\%$ ), and argon ( $\geq 99.998\%$ ) were purchased from BOC.

### 2.2. Apparatus and Procedure

The experiments were carried out in a 300 mL stirred autoclave (PARR model4566). The temperature inside the reactor was controlled by an oil bath heating circulator (IKA CBC5-Control) connected to the reactor's jacket. Previous work investigated different molecular weights for PLA methanolysis and concluded that the rate of degradation is independent of molecular weight [24]. Therefore, only one molecular weight of PLA was used for the reactions (Ingeo™ 6202D).

For the mixed catalyst methanolysis experiments in Section 3.1, 2 g of PLA, 10 mL of MeOH, 40 mL of THF, and various ratios of ZnAc and DMAP ranging from 0 to 0.1 g (total 5 wt %) were charged in the reactor. Various stirring speeds ranging from 0 to 700 rpm were also investigated. Once the reactor was charged, the autoclave was sealed and degassed with N<sub>2</sub> for at least 10 min before bringing the reactor to the desired working temperature (130 °C) at stirring speed ranging from 0 to 700 rpm. The reactor was left at 130 °C for a further 10 min to ensure all the PLA pellets were dissolved before 10 mL of MeOH was fed into the reactor via an HPLC pump at a rate of 10 mL min<sup>−1</sup>. Samples were taken periodically and tested by gas chromatograph (GC).

For the experiments in Section 3.2, for each MeOH experiment, 2 g of PLA, 10 mL of MeOH, 40 mL of THF, and 0.05 g ZnAc + 0.05 g DMAP (total 5 wt %) were charged in the reactor. In each EtOH experiment, 2 g of PLA, 14.5 mL of EtOH, 35.5 mL THF, and 0.05 g ZnAc + 0.05 g DMAP (total 5 wt %) were charged in the reactor. Once the reactor was charged, the autoclave was sealed and degassed with N<sub>2</sub> for at least 10 min before bringing the reactor to the desired working temperature (100–130 °C) at a stirring speed of 300 rpm. The reactor was left at the desired temperature for a further 10 min to ensure that all the PLA pellets were dissolved; then, either 10 mL of MeOH or 14.5 mL EtOH was fed into the reactor via an HPLC pump at a rate of 10 mL min<sup>−1</sup>. The volume of the two alcohols was varied to ensure both MeOH and EtOH experiments have ≈9 equivalents of alcohol per ester bond of PLA. Then, the volume of THF was adjusted to ensure the same concentration of PLA in both MeOH and EtOH experiments. Samples were taken periodically and tested by GC.

The experiments in Section 3.3 followed the same protocol as the MeOH experiments in Section 3.2. Samples were taken periodically and tested by <sup>1</sup>H NMR analysis.

### 2.3. GC and NMR

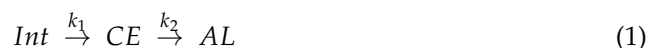
AL concentration was assessed by a GC coupled with Flame-Ionisation Detection (FID) (Agilent Technologies, Santa Clara, CA, USA, 6890N). Samples were injected by an autosampler (Agilent Technologies, 7683B), to a 30 m × 0.32 mm ID, 0.25 µm film thickness HP-5 Agilent capillary column using helium as the carrier and make-up gas with the following conditions: inlet temperature of 150 °C, 1 µL of injection volume, 1:400 split ratio, 250 °C detector temperature, with an initial oven temperature of 65 °C (held for 4 min); then, 100 °C min<sup>−1</sup> ramp to 195 °C (held for 1 min), followed by 100 °C min<sup>−1</sup> ramp to 230 °C (held for 5 min). The initial flowrate was 0.8 mL min<sup>−1</sup> (held for 5 min); then, it was 100 mL min<sup>−1</sup> ramp to 3 mL min<sup>−1</sup> (held for 5 min). A multiple point external standard calibration curve was prepared using standard solutions covering the range of AL concentrations. A linear response of the detector was determined for MeLa and EtLa ( $R^2 = 0.998$  and  $0.998$ , respectively).

<sup>1</sup>H NMR spectra were measured using a 400 MHz Bruker Avance II spectrometer. Samples were dissolved in, and referenced to, CDCl<sub>3</sub>. The experiments were monitored by determining the relative concentrations of methine functional groups calculated from NMR spectra. The methine protons were considered to be in one of three different environments: internal methine (Int) (5.09–5.21 ppm), chain-end (CE) (4.30–4.39 ppm/5.09–5.21 ppm), or methyl lactate (MeLa) (4.23–4.29 ppm). Selectivities and yields of MeLa as a function of temperature are presented as well as the estimated kinetic parameters of the reaction.

### 2.4. Kinetic Modelling

The experimental data were modelled using the simplified two-step reaction mechanism shown below in Equation (1). The model is simplified from the previous paper by not assuming an equilibrium for the second step [22]. The equilibrium only becomes significant at temperatures below 90 °C, as lower temperatures favor the reverse equilibrium step. The alcohol in excess was not included in the model. Int represents the internal methines along the PLA chains, CE represents the chain end methines of the oligomer fragments from cleaved PLA chains, and AL represents the alkyl lactate methines of the product. The

rate equations were solved analytically and fitted to the experimental data using SigmaPlot. The ester groups along PLA chains are rapidly cleaved by the alcohol nucleophile into chain end molecules, which are represented by the rate constant  $k_1$ . Then, ester groups along the chain end molecules are continually cleaved by the alcohol nucleophile into smaller fragments. When the alcohol attacks an ester group adjacent to the chain end, the product AL forms (MeOH produces MeLa, EtOH produces EtLa), which is represented by the rate constant  $k_2$ .



$$\frac{d[Int]}{dt} = -k_1[Int] \quad (2)$$

$$\frac{d[CE]}{dt} = k_1[Int] - k_2[CE] \quad (3)$$

$$\frac{d[AL]}{dt} = k_2[CE] \quad (4)$$

### 3. Results

#### 3.1. Mixed Catalyst Methanolysis

Table 1 shows the results obtained from the methanolysis of PLA using mixtures of DMAP and ZnAc. Various amounts of catalyst (ZnAc and DMAP) were investigated as well as the stirring speed. The total weight of catalyst/s used in each experiment was kept constant at 0.1 g (5 wt % relative to PLA) and a constant temperature of 130 °C was used to allow for comparison for different catalyst mixtures. The weight of catalyst ZnAc and DMAP was tested at 0, 0.025, 0.05, 0.075, and 0.1 g. When both catalysts were used in a single experiment, the total weight was 0.1 g. MeLa conversions (%) were calculated from GC concentration of MeLa and the theoretical max concentration of MeLa. Initial rates of production of MeLa were calculated from the concentration of MeLa divided by time taken at 60 min.

Comparing the initial rate of production of MeLa for both single catalyst reactions, using ZnAc outperformed DMAP by more than double the rate of MeLa production:  $5.53 \times 10^{-4} \text{ g mL}^{-1} \text{ min}^{-1}$  and  $2.45 \times 10^{-4} \text{ g mL}^{-1} \text{ min}^{-1}$ , respectively. If DMAP is used alongside ZnAc, the reaction rate increases significantly, suggesting a synergetic effect of the catalysts working together. This is considered a type II transformation, as either of the catalysts alone will lead to the formation of the final product but at a slower rate [40]. It is interesting to note that the 0.075 g ZnAc + 0.025 g DMAP experiment had a higher initial rate of production of MeLa than the 0.075 g DMAP + 0.025 g ZnAc experiment ( $8.38 \times 10^{-4} \text{ g mL}^{-1} \text{ min}^{-1}$  and  $8.2 \times 10^{-4} \text{ g mL}^{-1} \text{ min}^{-1}$  respectively). This observation along with the single catalyst results suggests that ZnAc is a more active catalyst for PLA methanolysis than DMAP. Using an equal amount of both catalysts elicited the highest initial rate of production of MeLa, and it achieved an 86% MeLa conversion in the quickest time, suggesting that the synergetic effect is strongest when there is an equal ratio of both catalysts. Both catalysts work by coordinating with the nucleophilic alcohol and the ester groups along PLA. They are partially cooperative as they both compete to coordinate with the alcohol molecules and ester groups. Since there is a surplus of alcohol and ester groups in comparison to catalyst molecules, their competition to coordinate becomes negligible. The catalyst mechanisms and economic benefit of using a dual catalyst system will be described further in the discussion.



**Table 1.** Methanolysis of PLA at 130 °C and 300 rpm, effect of different amounts of catalyst on final time (min), final MeLa conversion (%), time taken to reach 86% MeLa conversion, and initial rate of production of MeLa ( $\text{g mL}^{-1} \text{min}^{-1}$ ).

Catalyst (Total 0.1 g, 5 wt %)		Final Time (min)	Final MeLa Conversion (%)	Time Taken to Reach 86% MeLa Conversion (min)	Initial Rate of Production of MeLa ( $\text{g mL}^{-1} \text{min}^{-1}$ )
DMAP	ZnAc				
0.1	0	300	86	300	$2.45 \times 10^{-4}$
0.075	0.025	80	94	63	$8.20 \times 10^{-4}$
0.05	0.05	80	97	57	$8.50 \times 10^{-4}$
0.025	0.075	120	99	59	$8.38 \times 10^{-4}$
0	0.1	180	89	168	$5.53 \times 10^{-4}$

Table 2 shows the results obtained from the methanolysis of PLA using 0.025 g DMAP and 0.075 g ZnAc at 130 °C at different stirring speeds. MeLa conversions (%) were calculated from GC concentration of MeLa and the theoretical max concentration of MeLa. Initial rates of production of MeLa were calculated from the concentration of MeLa divided by time taken at 60 min. A stirring speed of 0 rpm generated a higher initial production of MeLa  $7.15 \times 10^{-4} \text{ g mL}^{-1} \text{min}^{-1}$  than 200 rpm and 400 rpm  $4.95 \times 10^{-4} \text{ g mL}^{-1} \text{min}^{-1}$  and  $6.27 \times 10^{-4} \text{ g mL}^{-1} \text{min}^{-1}$  respectively. Increasing the stirring speed above 400 rpm to 700 rpm increased the reaction rate to  $7.3 \times 10^{-4} \text{ g mL}^{-1} \text{min}^{-1}$ ; however, the highest rate was achieved at 300 rpm  $8.38 \times 10^{-4} \text{ g mL}^{-1} \text{min}^{-1}$ . In the case of stirring speed 0 rpm, there could be a large temperature gradient from the walls of the reactor to the reaction mixture; then, the chemical reaction would proceed faster near the reactor walls. This could explain the relatively short time taken to reach 86% MeLa conversion at 0 rpm. There was no clear trend with the effect of stirring speed on the reaction, so we decided to use 300 rpm for the proceeding experiments as it reached 86% MeLa conversion in the shortest time.

**Table 2.** Methanolysis of PLA at 130 °C 0.025 g DMAP + 0.075 g ZnAc, effect of different stirring speeds on final time (min), final MeLa conversion (%), time taken to reach 86% MeLa conversion, initial rate of production of MeLa ( $\text{g mL}^{-1} \text{min}^{-1}$ ).

Stirring Speed (rpm)	Final Time (min)	Final MeLa Conversion (%)	Time Taken to Reach 86% MeLa Conversion (min)	Initial Rate of Production of MeLa ( $\text{g mL}^{-1} \text{min}^{-1}$ )
0	120	93	92	$7.15 \times 10^{-4}$
200	180	87	175	$4.95 \times 10^{-4}$
300	120	99	59	$8.38 \times 10^{-4}$
400	120	95	96	$6.27 \times 10^{-4}$
700	90	93	78	$7.30 \times 10^{-4}$

### 3.2. Rate of Production of Alkyl Lactate

Table 3 shows the GC results of PLA alcoholysis experiments using MeOH and EtOH as the alcohol nucleophile. First, 0.05 g of each catalyst ZnAc and DMAP (total 5 wt % relative to PLA) were used in each experiment as well as a stirring speed of 300 rpm. AL conversions (%) were calculated from the GC data, and the theoretical max of concentration of MeLa/EtLa. The initial rate of production of AL was calculated from the concentration of AL divided by time taken at 60 min.

Comparing the results for both types of alcoholysis reactions at the same temperature, MeOH reactions have both a higher initial AL production rate and reach final conversions of AL in shorter times than for EtOH. The lower reactivity of EtOH can be explained by its increased steric hinderance of its nucleophilic attack in comparison to MeOH [41,42]. There is also a clear relationship in both types of alcoholysis reactions in that a higher temperature has a higher initial rate of AL production and reaches final AL yields in quicker times. This can simply be explained by the increased kinetic energy of the molecules at a higher temperature, so greater rates of successful collisions between molecules and a faster overall reaction. There is a greater difference in the initial rate of production of AL at

higher temperature repeats in comparison to lower temperature repeats; e.g., the difference between the initial rates of MeOH reactions at 130 °C is  $0.73 \times 10^{-4} \text{ g mL}^{-1} \text{ min}^{-1}$ , whereas the difference between MeOH reactions at 110 °C is only  $0.27 \times 10^{-4} \text{ g mL}^{-1} \text{ min}^{-1}$  and the difference between 100 °C reactions is 0.

**Table 3.** PLA alcoholysis using MeOH and EtOH, 0.05 g of DMAP, and 0.05 g of ZnAc at 300 rpm. Table shows initial rate of production for AL and time taken to reach final AL conversion (%) at different temperatures.

Alcohol	Temperature (°C)	Final Time (min)	Final AL Conversion (%)	Initial Rate of Production of AL ( $\text{g mL}^{-1} \text{ min}^{-1}$ )
MeOH	130	80	97	$8.10 \times 10^{-4}$
MeOH	130	120	99	$7.37 \times 10^{-4}$
MeOH	120	140	99	$5.27 \times 10^{-4}$
MeOH	120	120	96	$6.30 \times 10^{-4}$
MeOH	110	180	96	$4.45 \times 10^{-4}$
MeOH	110	240	90	$4.18 \times 10^{-4}$
MeOH	100	420	83	$2.43 \times 10^{-4}$
MeOH	100	420	81	$2.43 \times 10^{-4}$
EtOH	130	180	99	$5.15 \times 10^{-4}$
EtOH	130	180	99	$4.93 \times 10^{-4}$
EtOH	120	240	99	$4.50 \times 10^{-4}$
EtOH	120	240	99	$4.58 \times 10^{-4}$
EtOH	110	420	78	$1.81 \times 10^{-4}$

### 3.3. Conversion, Selectivity, and Yield of Methyl Lactate during PLA Methanolysis

Reaction progress was determined by the relative concentration of each methine functional group; this was achieved via  $^1\text{H}$  NMR spectroscopy where reaction samples were dissolved in  $\text{CDCl}_3$ . Each methine functional group was in one of three different environments, Int (5.09–5.21 ppm), CE (4.30–4.39 ppm/5.09–5.21 ppm), or MeLa (4.23–4.29 ppm). Figure 2 below shows stacked spectra for a 120 °C methanolysis experiment. The CE methine will always have two different chain ends of equal concentration. This allowed for the determination of the CE in the shared integral with the Int methine at 5.09–5.21 ppm, since it will be the same percentage as the lone CE integral at 4.30–4.39 ppm.

Table 4 shows the results of  $^1\text{H}$  NMR methanolysis experiments at 60 min. Conversion of Int groups ( $X_{\text{Int}}$ ), MeLa selectivity ( $S_{\text{MeLa}}$ ), and MeLa yield ( $Y_{\text{MeLa}}$ ) were calculated according to

$$X_{\text{Int}} = \frac{\text{Int}_0 - \text{Int}}{\text{Int}_0} \quad (5)$$

$$S_{\text{MeLa}} = \frac{\text{MeLa}}{\text{Int}_0 - \text{Int}} \quad (6)$$

$$Y_{\text{MeLa}} = S_{\text{MeLa}} X_{\text{Int}} \quad (7)$$

where  $\text{Int}_0$  is the initial concentration of the Int groups (100%). Averages for Int conversion, MeLa selectivity, and MeLa yield were taken for the same temperature experiments to allow for easier comparison. Although there is some variation in the results at each temperature, there is a clear trend that as temperature increases, so does the percentage of Int conversion, MeLa selectivity, and MeLa yield. The trend is clearer when looking at the averaged results. This can simply be explained since a higher temperature will raise the average kinetic energy of the reactant molecules; thus, a greater proportion of molecules will have sufficient energy to overcome the activation energy of the reaction, which is in accordance with the Arrhenius effect. By 130 °C, conversion of Int methine groups of the PLA chains into oligomers with chain end methines had reached  $\approx 100\%$ . The selectivity and yield of MeLa is  $\approx 70\%$  at 130 °C, meaning that the remaining 30% is chain-end methine oligomers. As the temperature decreases, the difference between MeLa selectivity and yield increases.



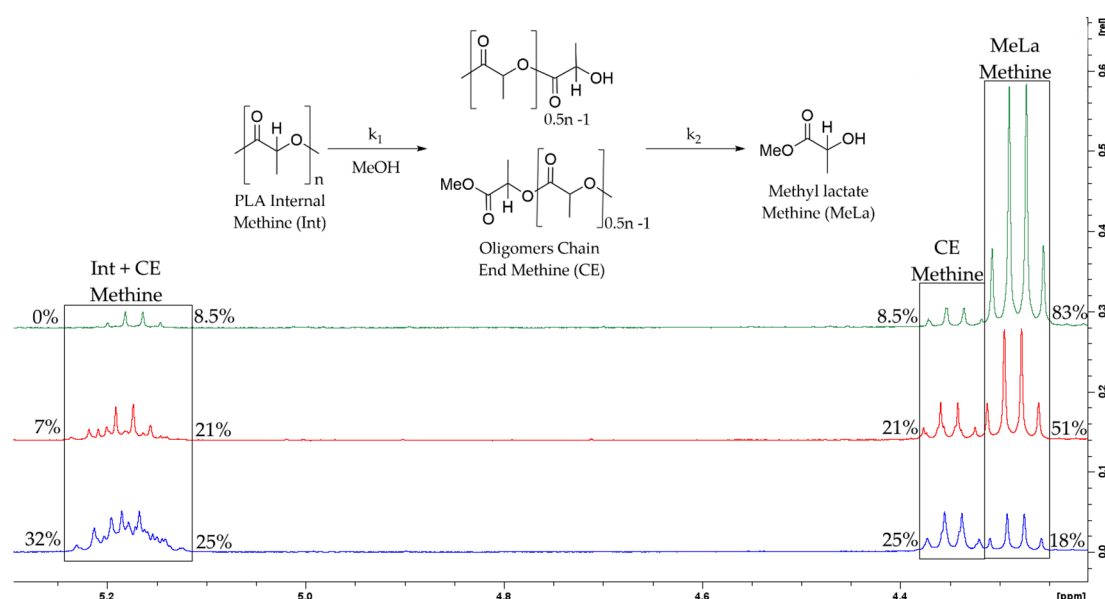


**Figure 2.**  $^1\text{H}$  NMR ( $\text{CDCl}_3$ , 400 MHz) stacked spectra of a methanolysis reaction at  $120^\circ\text{C}$  and the relative percentage of each methine Int, CE, and MeLa (blue spectrum 11 min, red spectrum 60 min, green spectrum 140 min).

**Table 4.** PLA methanolysis at 300 rpm with 0.05 g DMAP and 0.05 g ZnAc, conversion of Int groups, MeLa selectivity, and MeLa yield at different reaction temperatures.

Experiment Number	Temperature ( $^\circ\text{C}$ )	$X_{\text{Int}}$ (%)	$S_{\text{MeLa}}$ (%)	$Y_{\text{MeLa}}$ (%)	Average $X_{\text{Int}}$ (%)	Average $S_{\text{MeLa}}$ (%)	Average $Y_{\text{MeLa}}$ (%)
1	130	100	72	72	99.5	70.0	69.5
2	130	99	68	67			
3	120	93	55	51	95.0	56.5	53.5
4	120	97	58	56			
5	110	90	50	45	90.0	47.3	42.7
6	110	87	44	38			
7	110	93	48	45			
8	100	70	36	25	79.0	40.0	32.0
9	100	90	48	43			
10	100	77	36	28			

$X_{\text{Int}}$ ,  $S_{\text{MeLa}}$ ,  $Y_{\text{MeLa}}$  are determined at 60 min of reaction.

### 3.4. Arrhenius Temperature-Dependent Parameters

Relative concentrations of Int, CE, and MeLa methine groups were generated from  $^1\text{H}$  NMR spectra for each experiment. Using SigmaPlot, the relative concentrations of the methine groups were fitted to the simplified kinetic model described in Equation (1). Two typical reaction profiles are shown in Figure 3. The resulting rate constants from the fitted  $^1\text{H}$  NMR plots are shown Table 5. At all temperatures,  $k_1$  is greater than  $k_2$ ; therefore, Int methines are rapidly converted into CE methines, which slowly forms MeLa methines; step 2 is the rate-determining step of the overall reaction. Step 1 appears to be more sensitive to temperature change than step 2; there is a greater range in values for  $k_1$  than  $k_2$ . Decreasing the temperature decreases the difference in value between  $k_1$  and  $k_2$ . The kinetic fits are well matched with the fits from previous work of the authors, and the rate constants have the same order of magnitude [22].

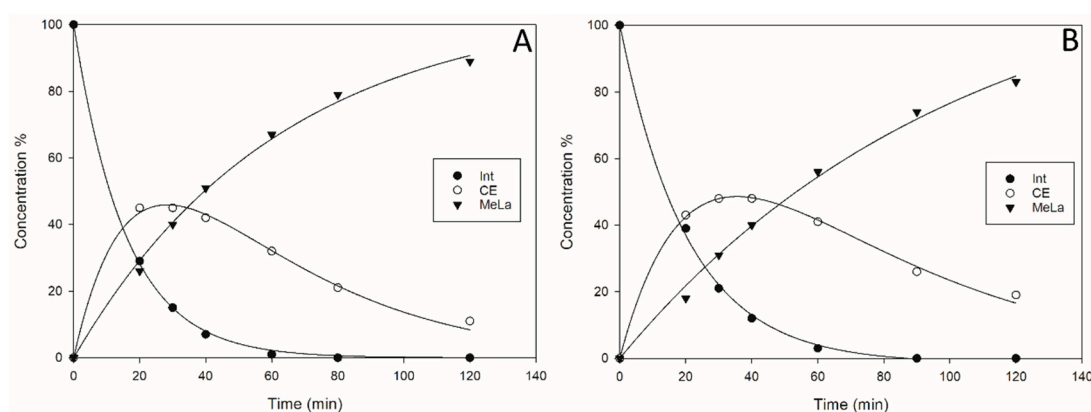


**Figure 3.** Reaction profiles obtained from  $^1\text{H}$  NMR data for methanolysis fitted in SigmaPlot. (A) 130 °C  $R^2 = 0.9943$  (B) 120 °C  $R^2 = 0.9954$ .

**Table 5.** Rate coefficients for each experiment, catalysed by ZnAc and DMAP.

Experiment Number	Temperature (°C)	$k_1$ (min $^{-1}$ )	$k_2$ (min $^{-1}$ )
1	130	$0.0858 \pm 0.0078$	$0.0274 \pm 0.0017$
2	130	$0.0445 \pm 0.0020$	$0.0275 \pm 0.0007$
3	120	$0.0717 \pm 0.0137$	$0.0175 \pm 0.0024$
4	120	$0.0378 \pm 0.0013$	$0.0203 \pm 0.0005$
5	110	$0.0289 \pm 0.0028$	$0.0143 \pm 0.0010$
6	110	$0.0224 \pm 0.0013$	$0.0111 \pm 0.0004$
7	110	$0.0217 \pm 0.0021$	$0.0122 \pm 0.0010$
8	100	$0.0114 \pm 0.0015$	$0.0079 \pm 0.0008$
9	100	$0.0152 \pm 0.0017$	$0.0103 \pm 0.0006$
10	100	$0.0138 \pm 0.0016$	$0.0070 \pm 0.0005$

The rate coefficients selected from Table 5 were used to generate the Arrhenius plots for PLA methanolysis shown in Figure 4. The entries selected from Table 5 were as follows: entry 1, the average of entry 3 and 4, entry 5, and entry 9, as they produced the best fit and  $R^2$  value for the resulting Arrhenius plots. According to Equation (1), the alcoholysis of PLA occurs in two steps: first, the PLA ester groups are cleaved by the alcohol into two chain end molecules with a rate coefficient of  $k_1$ . The second step involves the alcohol nucleophile attacking ester groups of the chain end molecule until the product alkyl lactate is formed with a rate coefficient of  $k_2$ . The activation energies for each step were obtained from the gradients of the Arrhenius plots.

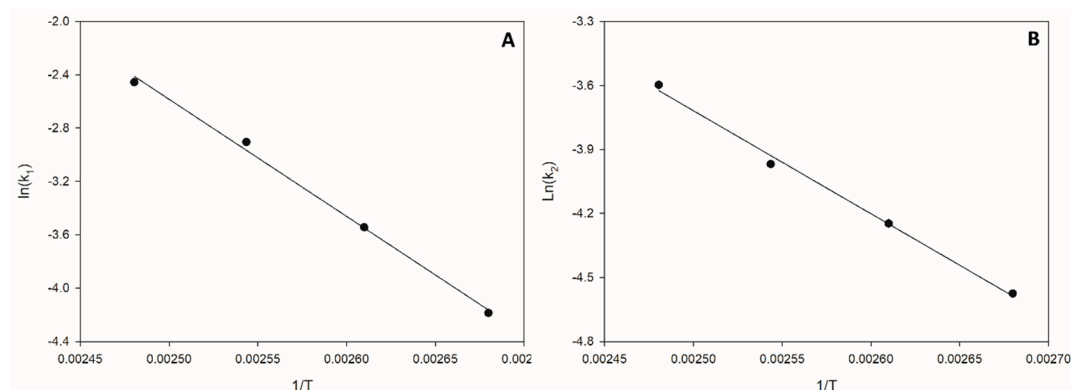


**Figure 4.** Arrhenius plots for methanolysis reactions at 130–100 °C, the best rate coefficients were selected from Table 4. (A)  $k_1$   $y = -8784.9x + 19.379$   $R^2 = 0.9963$  (B)  $k_2$   $y = -4829.9x + 8.357$   $R^2 = 0.9953$ .

Table 6 below shows the activation energy for each reaction step generated from the gradient of the Arrhenius plots; the values are comparable to literature values [24]. Figure 4A has a steeper slope than 4B; the reaction rate of step 1 is more sensitive to temperature change than step 2. This can be explained, since the nucleophilic attack of the alcohol towards the PLA ester groups is more sterically hindered by large PLA chains in comparison to nucleophilic attack towards chain end esters, which are smaller molecules. Thus, a higher temperature is required to give the alcohol sufficient kinetic energy for collision to overcome the steric hindrance of a larger chain, so step one has the larger activation energy. It is important to consider that the catalysts need to coordinate to both the alcohol and the ester groups for transesterification to occur; a less sterically hindered ester group will be easier to coordinate to and will then allow the catalyst to bring the alcohol in closer for nucleophilic attack.

**Table 6.** The activation energies for each step of PLA methanolysis.

Catalysts	Temperature (°C)	Ea <sub>1</sub> (kJ mol <sup>−1</sup> )	Ea <sub>2</sub> (kJ mol <sup>−1</sup> )
0.5 g ZnAc + 0.5 g DMAP	100–130	73.00 ± 13.57	40.16 ± 8.41

#### 4. Discussion

Alcoholysis of PLA via MeOH has higher initial rates of reaction than alcoholysis via EtOH. The lower reactivity of EtOH can be explained by the increased steric hindrance of its longer carbon chain, which impedes its coordination to the catalysts and its nucleophilic attack towards the ester groups along PLA [41,42]. A higher reaction temperature was found to increase the initial rate of production of AL, as shown in Table 3. A higher reaction temperature will raise the average kinetic energy of the reactant molecules; thus, a greater proportion of molecules will have sufficient energy to overcome the activation energy barrier, which explains the increases in production of AL with temperature. A higher reaction temperature was also shown in Table 4 to increase the average  $X_{Int}$  (%), average  $S_{MeLa}$  (%), and average  $Y_{MeLa}$  (%). An increase in  $X_{Int}$  (%) with temperature is straightforward; greater kinetic energy of reactant molecules leads to more collisions with PLA ester groups, and thus,  $X_{Int}$  (%) increases with temperature. Although the simplified two-step mechanism shown in Equation (1) has been used to obtain the activation energy, it fails to explain why  $S_{MeLa}$  (%) increases with temperature. If the second step is considered to be an equilibrium step, then the reverse reaction is favored at lower temperatures, while the forward reaction is favored at higher temperatures [22]. Therefore, as temperature increases, the forward equilibrium step is favored, increasing the production of MeLa and thus increasing the  $S_{MeLa}$  (%).

Organocatalysts such as DMAP have previously been shown to exhibit their catalytic activity through hydrogen bonding interactions involved in the depolymerisation mechanism [37,43–45]. Figure 5 shows how DMAP activates the alcohol nucleophile through hydrogen bonding while also coordinating to a PLA ester group. ZnAc has been shown to initiate transesterification reactions through a mechanism that involves the initial coordination to the alcohol nucleophile: a carboxylate shift followed by coordination to the ester group [46,47]. Figure 6 shows that this mechanism, ZnAc takes on a six-coordinate structure with its ligands approximately octahedral around the Zn(II) ion [48].

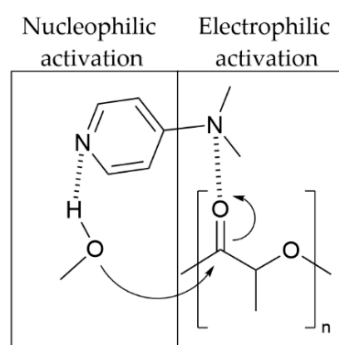


**Figure 5.** DMAP coordination to methanol and a PLA ester group during methanolysis.

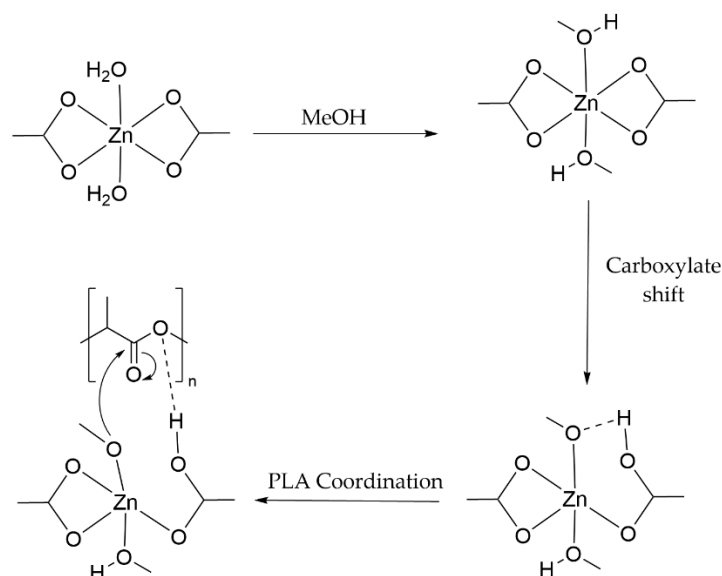


**Figure 6.** ZnAc coordination to methanol followed by a carboxylate shift and coordination to a PLA ester group during methanolysis, adapted from [46].

According to Equation (1), the first step of the alcoholysis reaction is the initial cleavage of the PLA chain; this step is represented by the coefficient  $k_1$ . The alcohol nucleophile randomly attacks an ester group along the PLA chain, causing a transesterification reaction that generates two CE oligomer molecules for each cleavage. After the initial cleavage, multiple chain scission reactions occur where the alcohol nucleophile continues to cleave ester linkages along PLA chains and the oligomer fragments. When the alcohol nucleophile attacks an ester linkage adjacent to a CE group, the value-added product AL forms; this is step two of the overall reaction and is represented by  $k_2$ . The reaction scheme for PLA methanolysis using both catalysts is shown below in Figure 7.

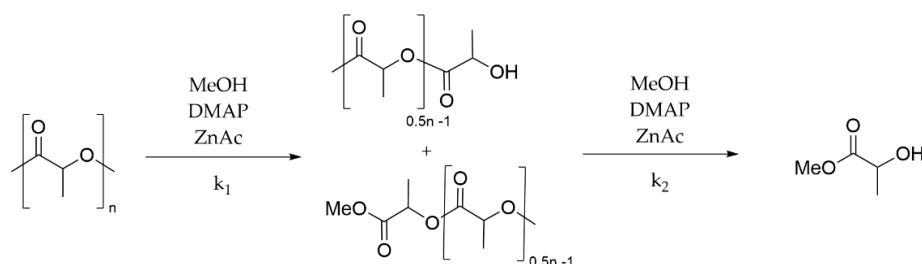


**Figure 7.** Reaction scheme for methanolysis of PLA, using DMAP and ZnAc as catalysts.

At all temperatures,  $k_1$  is greater than  $k_2$ ; this means that the ester groups of the PLA chains are rapidly cleaved into CE oligomers, which then build up in the system. Over a

period of time, the CE oligomers are slowly converted into the product AL, as this step is the rate-determining step of the overall reaction. Step 1 appears to be more sensitive to temperature change, and as the temperature decreases, the difference between  $k_1$  and  $k_2$  decreases. The greater sensitivity to temperature is shown by the activation energy for step 1 ( $73.00 \pm 13.57 \text{ kJ mol}^{-1}$ ) being higher than that for step 2 ( $40.16 \pm 8.41 \text{ kJ mol}^{-1}$ ).

The higher activation energy of step 1 is also expected when considering the mechanism. For catalytic alcoholysis to occur, either catalyst will need to coordinate to both the alcohol nucleophile and the ester group of either a PLA chain or an oligomer chain. Coordination to an ester group belonging to PLA can be thought to be more sterically hindered than an ester group belonging to a smaller chained oligomer fragment. Therefore, a higher temperature will be needed in order for the alcohol nucleophile to have a successful collision with the ester group of PLA, and thus, step 1 has the higher activation energy barrier. Although DMAP and ZnAc differ in mechanism—DMAP exhibiting its catalytic activity through hydrogen bonding interactions and ZnAc carboxylate shifting before coordinating to the ester groups—both catalysts need to coordinate to the ester group [43,44,46,47]. Despite both catalysts competing to coordinate to the same alcohol molecules and ester groups, their competition is negligible, since these are both in excess in comparison with the fewer catalyst molecules. After an alcohol ligand on ZnAc carboxylate shifts, it becomes a stronger nucleophile in comparison to an alcohol hydrogen bonded to DMAP, which explains the results that ZnAc is more activating towards PLA alcoholysis than DMAP [46].

Out of the two product lactates, EtLa is considered the more useful and has the highest demand; however, MeLa has a greater commercial value [49,50]. Since MeLa is more valuable than EtLa, we have done an estimation, which shows that dual catalytic methanolysis of PLA is more economically advantageous than single catalyst methanolysis. To simplify the estimation, the cost of product purification is ignored. The process is economically valuable as long as the cost of reagents and operating costs is less than the yield and value of the product. At the time of publication, the chemical prices listed on Sigma Aldrich were as follows: Methyl DL-lactate 5 mL (5.45 g) = £45, DMAP 5 g = £11.6, ZnAc 250 g = £34, MeOH 1 L = £24. NatureWorks PLA pellets can be purchased online through a third party at 1 kg = £3.55. The cost of reagents for a single experiment: DMAP 0.05 g = £0.116, ZnAc 0.05 g = £0.0068, MeOH 10 mL = £0.24, PLA 2 g = £0.0071. The total costs of reagents for a single ZnAc/DMAP experiment is ≈£0.37. The oil bath heater has a power usage of 3 kWh and electricity costs ≈15p per kWh. 2 g (PLA)/72.06 g mol<sup>-1</sup> (ester repeat unit) = 0.0278 mol of ester groups, 0.0278 mol × 104.1 g mol<sup>-1</sup> (Molecular weight of MeLa) = 2.89 g MeLa (100% yield).

According to Table 4, at 130 °C, 100% conversion of ester groups gives an MeLa yield of ≈70%. Comparing two experiments from Table 1 using only ZnAc achieved 89% ester conversion in 180 min, whereas, using an equal ratio of ZnAc and DMAP achieved 97% ester conversion in 80 min. Assuming that the MeLa yield scales equally with ester conversion; the ZnAc experiment at 89% ester conversion would have an MeLa yield of ≈59%, the equal ratio of ZnAc and DMAP experiment at 97% ester conversion would have an MeLa yield of ≈67%. The ZnAc experiment would have an input cost of £0.26 (Reagents) + £1.35 (9 kWh) to generate a 59% yield MeLa ≈ 1.71 g (£14.12), which is a profit of £12.51. The ZnAc/DMAP experiment would have an input cost of £0.37 (Reagents) + £0.60 (4 kWh) to generate a 67% yield MeLa ≈ 1.94 g (£16.02), which is a profit of £15.05. Although the ZnAc/DMAP is only slightly more profitable than ZnAc alone, the fact that the reaction is much quicker means over time it will be much more profitable. ZnAc/DMAP has a profit per hour of £11.29 vs ZnAc alone which has a profit per hour of £6.26.

In order for this reaction to be industrially viable, the reaction would have to be scaled up in order to increase the yield of MeLa. Both catalysts would need to be immobilised onto a solid support; thus, recovery of the catalysts from the product no longer becomes an issue [51,52]. Additionally, distillation would need to be used in order to recover THF and the remaining MeOH once the reaction has completed, after which MeLa would remain

in the reactor with oligomers. Since MeLa has a lower boiling point than the oligomers, it could be purified with further distillation. As long as the total cost of purification is less than the estimated profit, then this reaction is industrially viable, for recycling postconsumer PLA and for upscaling virgin PLA. Both ethanolysis and methanolysis are suitable for a circular economy approach as postconsumer PLA could be turned into a value-added product AL; additionally, ALs could be converted to lactide and repolymerised to PLA [27,28]. Both routes would be much better than landfilling and better than composting PLA as the energy stored in its molecular structure would be recovered [21].

## 5. Conclusions

This work has shown that there is a synergistic effect of using two transesterification catalysts together, ZnAc and DMAP, for the alcoholysis of PLA. Although ZnAc has a higher activity for the reaction than DMAP, together in an equal ratio produces the highest reaction rate. This synergistic effect could be exploited on an industrial scale as both catalysts are cheap and commercially available. Alcoholysis of PLA proceeds faster in MeOH than EtOH, MeOH is the stronger nucleophile, as it is less sterically hindered due to its smaller carbon chain. Chemically recycling via alcoholysis provides an excellent route to recycle the end-of-life PLA to obtain value-added ALs. Of the two ALs produced, EtLa has the highest demand; however, methanolysis proceeds much faster and MeLa has a greater commercial value. Either route would be utilising a circular economy as postconsumer PLA would be recycled into products of equivalent functionality. Additionally, either of the lactates could be converted into lactide for the repolymerisation of virgin PLA if it were desired. The estimated activation energy for the first and second step of methanolysis was calculated at 73.00 kJ mol<sup>−1</sup> and 40.16 kJ mol<sup>−1</sup> respectively.

**Author Contributions:** Conceptualization, F.M.L. and J.W.; methodology, F.M.L.; validation, F.M.L.; formal analysis, F.M.L.; investigation, F.M.L.; resources, F.M.L. and J.W.; data curation, F.M.L.; writing—original draft preparation, F.M.L.; writing—review and editing, F.M.L., A.I. and J.W.; visualization, F.M.L.; supervision, A.I. and J.W.; project administration, J.W.; funding acquisition, J.W. All authors have read and agreed to the published version of the manuscript.

**Funding:** This research was funded by ESPRC, grant number EP/P016405/1.

**Institutional Review Board Statement:** Not applicable.

**Informed Consent Statement:** Not applicable.

**Data Availability Statement:** Data associated with this paper are available free of charge via [edata.bham.ac.uk](http://edata.bham.ac.uk).

**Acknowledgments:** NatureWorks LLC are acknowledge for their donation of PLA samples. F.M.L. is grateful to the School of Chemical Engineering at University of Birmingham for a studentship.

**Conflicts of Interest:** The authors declare no conflict of interest.

## References

1. World Economic Forum. *The New Plastics Economy Rethinking the Future of Plastics*; World Economic Forum: Colony, Switzerland, 2016; pp. 1–36.
2. Geyer, R. *Production, Use, and Fate of Synthetic Polymers*; Elsevier BV: Amsterdam, The Netherlands, 2020; pp. 13–32. ISBN 9780128178805.
3. Geyer, R.; Jambeck, J.R.; Law, K.L. Production, use, and fate of all plastics ever made. *Sci. Adv.* **2017**, *3*, e1700782. [[CrossRef](#)] [[PubMed](#)]
4. Hahladakis, J.N.; Iacovidou, E. Closing the loop on plastic packaging materials: What is quality and how does it affect their circularity? *Sci. Total Environ.* **2018**, *630*, 1394–1400. [[CrossRef](#)] [[PubMed](#)]
5. Liu, Z.; Adams, M.; Cote, R.P.; Chen, Q.; Wu, R.; Wen, Z.; Liu, W.; Dong, L. How does circular economy respond to greenhouse gas emissions reduction: An analysis of Chinese plastic recycling industries. *Renew. Sustain. Energy Rev.* **2018**, *91*, 1162–1169. [[CrossRef](#)]
6. Dilkes-Hoffman, L.S.; Pratt, S.; Lant, P.A.; Laycock, B. The Role of Biodegradable Plastic in Solving Plastic Solid Waste Accumulation. In *Plastics to Energy*; Elsevier BV: Amsterdam, The Netherlands, 2019; pp. 469–505. ISBN 9780128131404.



7. Eriksen, M.K.; Christiansen, J.D.; Daugaard, A.E.; Astrup, T.F. Closing the loop for PET, PE and PP waste from households: Influence of material properties and product design for plastic recycling. *Waste Manag.* **2019**, *96*, 75–85. [\[CrossRef\]](#)
8. Ragaert, K.; Delva, L.; van Geem, K. Mechanical and chemical recycling of solid plastic waste. *Waste Manag.* **2017**, *69*, 24–58. [\[CrossRef\]](#)
9. Sudhakar, M.; Trishul, A.; Doble, M.; Kumar, K.S.; Jahan, S.S.; Inbakandan, D.; Viduthalai, R.; Umadevi, V.; Murthy, P.S.; Venkatesan, R. Biofouling and biodegradation of polyolefins in ocean waters. *Polym. Degrad. Stab.* **2007**, *92*, 1743–1752. [\[CrossRef\]](#)
10. Zhang, C.; Chen, X.; Wang, J.; Tan, L. Toxic effects of microplastic on marine microalgae *Skeletonema costatum*: Interactions between microplastic and algae. *Environ. Pollut.* **2017**, *220*, 1282–1288. [\[CrossRef\]](#)
11. Sekerci, Y.; Petrovskii, S. Global Warming Can Lead to Depletion of Oxygen by Disrupting Phytoplankton Photosynthesis: A Mathematical Modelling Approach. *Geosciences* **2018**, *8*, 201. [\[CrossRef\]](#)
12. Confente, I.; Scarpi, D.; Russo, I. Marketing a new generation of bio-plastics products for a circular economy: The role of green self-identity, self-congruity, and perceived value. *J. Bus. Res.* **2020**, *112*, 431–439. [\[CrossRef\]](#)
13. Haider, T.P.; Völker, C.; Kramm, J.; Landfester, K.; Wurm, F.R. Plastics of the Future? The Impact of Biodegradable Polymers on the Environment and on Society. *Angew. Chem. Int. Ed.* **2019**, *58*, 50–62. [\[CrossRef\]](#) [\[PubMed\]](#)
14. European Bioplastics. *Bioplastics Facts and Figures*; European Bioplastics: Berlin, Germany, 2019.
15. Parker, K.; Garancher, J.-P.; Shah, S.; Fernyhough, A. Expanded polylactic acid—An eco-friendly alternative to polystyrene foam. *J. Cell. Plast.* **2011**, *47*, 233–243. [\[CrossRef\]](#)
16. California Department of Resources Recycling and Recovery. *PLA and PHA Biodegradation in the Marine Environment*; Department of Resources Recycling and Recovery: Sacramento, CA, USA, 2012; p. 1.
17. Tokiwa, Y.; Calabia, B.P. Biodegradability and Biodegradation of Polyesters. *J. Polym. Environ.* **2007**, *15*, 259–267. [\[CrossRef\]](#)
18. Shogren, R.L.; Doane, W.M.; Garlotta, D.; Lawton, J.W.; Willett, J.L. Biodegradation of starch/polylactic acid/poly(hydroxyester-ether) composite bars in soil. *Polym. Degrad. Stab.* **2003**, *79*, 405–411. [\[CrossRef\]](#)
19. Nampoothiri, K.M.; Nair, N.R.; John, R.P. An overview of the recent developments in polylactide (PLA) research. *Bioresour. Technol.* **2010**, *101*, 8493–8501. [\[CrossRef\]](#)
20. Niaounakis, M. Recycling of biopolymers—The patent perspective. *Eur. Polym. J.* **2019**, *114*, 464–475. [\[CrossRef\]](#)
21. Lamberti, F.M.; Román-Ramírez, L.A.; Wood, J. Recycling of Bioplastics: Routes and Benefits. *J. Polym. Environ.* **2020**, *28*, 2551–2571. [\[CrossRef\]](#)
22. Lamberti, F.M.; Román-Ramírez, L.; McKeown, P.; Jones, M.; Wood, J. Kinetics of Alkyl Lactate Formation from the Alcoholysis of Poly(Lactic Acid). *Processes* **2020**, *8*, 738. [\[CrossRef\]](#)
23. Román-Ramírez, L.A.; McKeown, P.; Jones, M.D.; Wood, J. Kinetics of Methyl Lactate Formation from the Transesterification of Polylactic Acid Catalyzed by Zn(II) Complexes. *ACS Omega* **2020**, *5*, 5556–5564. [\[CrossRef\]](#) [\[PubMed\]](#)
24. Román-Ramírez, L.A.; McKeown, P.; Jones, M.D.; Wood, J. Poly(lactic acid) Degradation into Methyl Lactate Catalyzed by a Well-Defined Zn(II) Complex. *ACS Catal.* **2019**, *9*, 409–416. [\[CrossRef\]](#)
25. Calvo-Flores, F.G.; Monteagudo-Arrebola, M.J.; Dobado, J.A.; Isac-García, J. Green and Bio-Based Solvents. *Top. Curr. Chem.* **2018**, *376*, 1–40. [\[CrossRef\]](#) [\[PubMed\]](#)
26. Biddy, M.J.; Scarlata, C.J.; Kinchin, C.M. *Chemicals from Biomass: A Market Assessment of Bioproducts with Near-Term Potential*; NREL: Golden, CO, USA, 2016. [\[CrossRef\]](#)
27. De Clercq, R.; Dusselier, M.; Poleunis, C.; Debecker, D.P.; Giebler, L.; Oswald, S.; Makshina, E.; Sels, B.F. Titania-Silica Catalysts for Lactide Production from Renewable Alkyl Lactates: Structure–Activity Relations. *ACS Catal.* **2018**, *8*, 8130–8139. [\[CrossRef\]](#)
28. De Clercq, R.; Dusselier, M.; Makshina, E.; Sels, B.F. Catalytic Gas-Phase Production of Lactide from Renewable Alkyl Lactates. *Angew. Chem. Int. Ed.* **2018**, *57*, 3074–3078. [\[CrossRef\]](#) [\[PubMed\]](#)
29. McKeown, P.; McCormick, S.N.; Mahon, M.F.; Jones, M.D. Highly active Mg(ii) and Zn(ii) complexes for the ring opening polymerisation of lactide. *Polym. Chem.* **2018**, *9*, 5339–5347. [\[CrossRef\]](#)
30. Alberti, C.; Enthaler, S. Depolymerization of End-of-Life Poly(lactide) to Lactide via Zinc-Catalysis. *ChemistrySelect* **2020**, *5*, 14759–14763. [\[CrossRef\]](#)
31. Sánchez, A.C.; Collinson, S.R. The selective recycling of mixed plastic waste of polylactic acid and polyethylene terephthalate by control of process conditions. *Eur. Polym. J.* **2011**, *47*, 1970–1976. [\[CrossRef\]](#)
32. Wang, C.-S.; Sun, Y.-M.; Hu, L.-C. Poly(ethylene naphthalate) formation 1. transesterification of dimethylnaphthalate with ethylene glycol. *J. Polym. Res.* **1994**, *1*, 131–139. [\[CrossRef\]](#)
33. Aiemsa-Art, C.; Phanwiroj, P.; Potiyaraj, P. Thermal and Morphological Properties of Polyurethane Foams Prepared from Microwave-assisted Glycolized Products of PET Bottles Wastes. *Energy Procedia* **2011**, *9*, 428–434. [\[CrossRef\]](#)
34. Sherwood, J. Closed-Loop Recycling of Polymers Using Solvents: Remaking plastics for a circular economy. *Johns. Matthey Technol. Rev.* **2019**, *64*, 4–15. [\[CrossRef\]](#)
35. Alberti, C.; Damps, N.; Meißner, R.R.R.; Enthaler, S. Depolymerization of End-of-Life Poly(lactide) via 4-Dimethylaminopyridine-Catalyzed Methanolysis. *ChemistrySelect* **2019**, *4*, 6845–6848. [\[CrossRef\]](#)
36. Alberti, C.; Scheliga, F.; Enthaler, S. Depolymerization of End-of-Life Poly(bisphenol A carbonate) via Transesterification with Acetic Anhydride as Depolymerization Reagent. *ChemistrySelect* **2019**, *4*, 2639–2643. [\[CrossRef\]](#)
37. Otera, J. Transesterification. *Chem. Rev.* **1993**, *93*, 1449–1470. [\[CrossRef\]](#)
38. Zhong, C.; Shi, X. When Organocatalysis Meets Transition-Metal Catalysis. *Eur. J. Org. Chem.* **2010**, *16*, 2999–3025. [\[CrossRef\]](#)

- 
39. Bin Kim, U.; Jung, D.J.; Jeon, H.J.; Rathwell, K.; Lee, S.-G. Synergistic Dual Transition Metal Catalysis. *Chem. Rev.* **2020**, *120*, 13382–13433. [[CrossRef](#)]
  40. Romiti, F.; del Pozo, J.; Paioti, P.H.S.; Gonsales, S.A.; Li, X.; Hartrampf, F.W.W.; Hoveyda, A.H. Different Strategies for Designing Dual-Catalytic Enantioselective Processes: From Fully Cooperative to Non-cooperative Systems. *J. Am. Chem. Soc.* **2019**, *141*, 17952–17961. [[CrossRef](#)] [[PubMed](#)]
  41. Petrus, R.; Bykowski, D.; Sobota, P. Solvothermal Alcoholysis Routes for Recycling Polylactide Waste as Lactic Acid Esters. *ACS Catal.* **2016**, *6*, 5222–5235. [[CrossRef](#)]
  42. Liu, F.; Guo, J.; Zhao, P.; Gu, Y.; Gao, J.; Liu, M. Facile synthesis of DBU-based protic ionic liquid for efficient alcoholysis of waste poly(lactic acid) to lactate esters. *Polym. Degrad. Stab.* **2019**, *167*, 124–129. [[CrossRef](#)]
  43. Jehanno, C.; Pérez-Madriral, M.M.; Demarteau, J.; Sardon, H.; Dove, A.P. Organocatalysis for depolymerisation. *Polym. Chem.* **2019**, *10*, 172–186. [[CrossRef](#)]
  44. Xu, S.; Held, I.; Kempf, B.; Mayr, H.; Steglich, W.; Zipse, H. The DMAP-Catalyzed Acetylation of Alcohols—A Mechanistic Study (DMAP=4-(Dimethylamino)pyridine). *Chem. A Eur. J.* **2005**, *11*, 4751–4757. [[CrossRef](#)] [[PubMed](#)]
  45. Thomas, C.; Bibal, B. Hydrogen-bonding organocatalysts for ring-opening polymerization. *Green Chem.* **2014**, *16*, 1687–1699. [[CrossRef](#)]
  46. Reinoso, D.M.; Ferreira, M.L.; Tonetto, G.M. Study of the reaction mechanism of the transesterification of triglycerides catalyzed by zinc carboxylates. *J. Mol. Catal. A Chem.* **2013**, *377*, 29–41. [[CrossRef](#)]
  47. Reinoso, D.M.; Damiani, D.E.; Tonetto, G.M. Zinc carboxylic salts used as catalyst in the biodiesel synthesis by esterification and transesterification: Study of the stability in the reaction medium. *Appl. Catal. A Gen.* **2012**, *449*, 88–95. [[CrossRef](#)]
  48. Ishioka, T.; Murata, A.; Kitagawa, Y.; Nakamura, K.T. Zinc(II) Acetate Dihydrate. *Acta Crystallogr. Sect. C Cryst. Struct. Commun.* **1997**, *53*, 1029–1031. [[CrossRef](#)]
  49. Pereira, C.S.M.; Silva, V.M.T.M.; Rodrigues, A.E. Ethyl lactate as a solvent: Properties, applications and production processes—A review. *Green Chem.* **2011**, *13*, 2658–2671. [[CrossRef](#)]
  50. Dorosz, U.; Barteczko, N.; Latos, P.; Erfurt, K.; Pankalla, E.; Chrobok, A. Highly Efficient Biphasic System for the Synthesis of Alkyl Lactates in the Presence of Acidic Ionic Liquids. *Catalysts* **2020**, *10*, 37. [[CrossRef](#)]
  51. Nava, R.; Halachev, T.; Rodríguez, R.; Castaño, V. Immobilized zinc acetate complex on the surface of silica–alumina gel modified by succinic acid: An efficient catalyst for the esterification of DMT. *Microporous Mesoporous Mater.* **2005**, *78*, 91–96. [[CrossRef](#)]
  52. Shaikh, I.R. Organocatalysis: Key Trends in Green Synthetic Chemistry, Challenges, Scope towards Heterogenization, and Importance from Research and Industrial Point of View. *J. Catal.* **2014**, *2014*, 1–35. [[CrossRef](#)]